

Chapter 2

Assessing Protein-Ultrafiltration Membrane Interactions Using Flow Field-Flow Fractionation

Galina E. Kassalainen and S. Kim Ratanathanawongs Williams

Abstract Flow FFF (FIFFF) is used to rapidly and conveniently measure initial stage protein fouling on ultrafiltration membranes. The procedures and findings are applicable to both ultrafiltration processes and flow FFF analyses. UV detector peak areas representing analytes eluting from the FIFFF channel are used to determine the amount of sample recovered. It was observed that compositionally similar membranes from different companies exhibited significantly different sample recoveries. The measured FIFFF retention times provided insights into the relationship between sample recovery and proximity of the sample layer to the membrane wall. Increasingly large amounts of bovine serum albumin were adsorbed when the average distance of the sample layer was less than 11 μm . This information can be used to establish guidelines for flowrates that should be used to minimize sample adsorption and membrane fouling. The methods described here also provide a means to rapidly test membranes when developing a new FIFFF analysis, evaluating membranes from different manufacturers, and testing batch-to-batch membrane reproducibility.

Keywords Flow FFF • Protein-membrane interactions • Membrane fouling • Adsorption • Ultrafiltration • Membrane performance • Membrane evaluation • Lactate dehydrogenase

G.E. Kassalainen • S.K.R. Williams (✉)

Laboratory for Advanced Separations Technologies, Department of Chemistry and Geochemistry, Colorado School of Mines, Golden, CO, USA

e-mail: krwillia@mines.edu

2.1 Introduction

Flow field-flow fractionation (FIFFF) has become the most widely used technique of the FFF family [1–5]. Reasons include the need for a low shear rate size-based separation for fragile and/or large analytes such as protein aggregates and complexes, the wide applicable size range that is ideal for polydisperse samples, and the straightforward relationship between retention time and hydrodynamic diameter [6–14]. These advantageous features originate from the open channel design intrinsic to FFF and the crossflow of fluid that is used to retain sample in FIFFF. This crossflow necessitates the use of semipermeable walls that allow permeation of fluid out of the channel in a direction perpendicular to the separation axis. Membranes are used to fulfill this function and present both challenges and opportunities. The selection of a suitable membrane is critical to the success of an FIFFF analysis. The ideal membrane would exhibit no undesirable interactions with the sample, the sample would be completely recovered, and accurate physicochemical properties would be calculated from the measured retention times using FFF theory. This is often not the case particularly when the samples analyzed have wide distributions of chemistries, charges, etc. The challenge is to identify the membrane and experimental conditions for optimum resolution and sample recovery. The use of a membrane in FIFFF channels also opens up new opportunities that have remained largely untapped. Primary among these is the role of FIFFF in studying analyte-membrane interactions. Since the separation process occurs at the surface of the membrane, FIFFF can be used as a sensitive probe to study interactions. Such studies can shed invaluable insights into membrane fouling in ultrafiltration (UF) processes and help establish guidelines for operational conditions. Furthermore, the short analysis times and the small amount of sample injected makes FIFFF an ideal method for quality control of UF membranes that are used for filtration and FIFFF.

This chapter commences with an example study of enzyme dissociation that highlights many of the advantages of FIFFF. The focus then shifts to the use of FIFFF to assess protein-ultrafiltration membrane interactions and the description of a simple method to test membrane suitability and select experimental conditions. This method for evaluating membrane performance is suitable for UF processes, FIFFF, and FFF in general.

2.2 Theory

Differential retention in FFF is based on the formation of equilibrium distributions of different sample components in different flow velocity streamlines of a parabolic flow (see Fig. 2.1). These equilibrium distributions are formed when sample is transported by an applied field U towards a so-called accumulation wall and the subsequent concentration build-up results in sample diffusion away from the wall

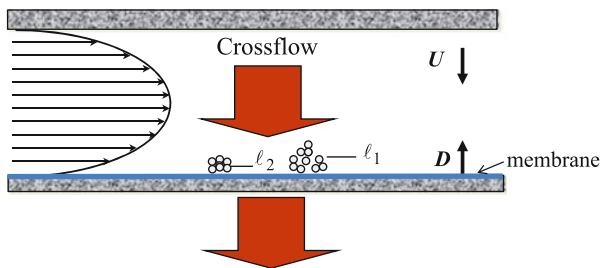


Fig. 2.1 FIFFF channel and separation mechanism

[1–5]. Each distribution can be described by an exponential concentration gradient and a unique mean layer thickness ℓ .

Figure 2.1 shows the distribution of two components in different velocity streamlines, as represented by ℓ_1 and ℓ_2 and the faster displacement of component 1. In the case of flow FFF, the field is provided by a second flow of fluid or crossflow that is driven perpendicular to the separation axis and exits through a semipermeable membrane situated on a porous frit panel. Since all components are positively displaced to this membrane wall irrespective of physicochemical properties, the differentiating sample property that leads to different equilibrium positions in the parabolic flow profile (and thus retention) is the diffusion coefficient D . The D and ℓ terms are related to experimental parameters by Eq. 2.1 which can be derived from the equations in Chap. 1.

$$t_r = \frac{wr^0}{6\ell} = \frac{w^2\dot{V}_c}{6D\dot{V}} \quad (2.1)$$

The t_r is measured retention time, \dot{V}_c is cross flowrate, \dot{V} is channel flowrate, w is channel thickness, and r^0 is void time. Hydrodynamic diameters can be calculated from D via the Stokes-Einstein equation ($D = kT/3\pi\eta d$ where k is the Boltzmann constant, T is temperature, η is carrier liquid viscosity, and d is hydrodynamic diameter). The basic principles of flow FFF are fully described in Chap. 1. Only aspects that are directly relevant to this chapter will be further highlighted.

2.3 Experimental

The FIFFF systems consisted of a channel (symmetric and asymmetric), two pumps for supplying the liquid flows (Model 414 HPLC, Kontron Electrolab, London, U.K. and Model HPLC 420, ESA Inc., Bedford, MA), a 25- μ L loop injector (Model 7010, Rheodyne, Inc., Cotati, CA), and a UV-detector (Model 757, Applied Biosystems, Ramsey, NJ). The flowrates were measured using two electronic balances (Model TS4000S, Ohaus, Florham Park, NJ) connected to the RS-232 ports of a PC computer. Inlet and outlet flow rates were equalized using a flow restrictor (Upchurch Scientific, Oak Harbor, CA) located at the detector outlet.

A three-way valve (Hamilton, Reno, NV) and a six-port valve (Valco E36, Chrom Tech, Apple Valley, MN) were used for changing flow paths during stop-flow relaxation and channel rinsing. The channel volume, cut out from the Mylar spacer, had a length of 28.5 cm tip-to-tip and a breadth of 2.0 cm. The UF membrane cross-section area inside the FIFFF channel was 53 cm^2 unless otherwise specified. The spacer thickness was $254 \text{ }\mu\text{m}$ but the actual thickness ranged between 210 and $245 \text{ }\mu\text{m}$ (measured using calipers). This smaller channel thickness is due to membrane compression in areas of contact with the spacer.

2.3.1 *Lactate Dehydrogenase Study*

The LDH-5 sample (6.7 mg/mL in 2.1 M $(\text{NH}_4)\text{SO}_4$, pH 6.0) was obtained from Sigma (St. Louis, MO, USA). Repeated dialysis was carried out with 0.2 M phosphate buffer at pH 7.6 to obtain the enzyme suspension subsequently used in AsFIFFF experiments. The LDH-5 concentration after dialysis and filtration of the precipitate was determined by UV absorbance at 280 nm and literature data (10 mg/mL gives $A = 14.6$ [15]) to be $\sim 3 \text{ mg/mL}$. A regenerated cellulose membrane with a 5 kDa molecular weight cut-off (Nadir, Wiesbaden, Germany) was used.

2.3.2 *Sample Adsorption Study*

Six commercial UF membranes composed of regenerated cellulose (RC) and poly (ethersulfone) (PES) were studied. They are designated as RC1(30 kDa), RC2 (110 kDa), RC3 (10 kDa), RC4 (5 kDa), PES1 (10 kDa), and PES2 (10 kDa) where the numbers in parenthesis are the nominal molecular weight cut-offs (MWCO). The carrier liquid was a 0.01 M Tham-boric acid buffer having a pH in the range of 7.3–9.0. Tham, or tris-(hydroxymethyl)aminomethane, was obtained from Fisher Scientific (Fair Lawn, NJ), and boric acid was obtained from VWR Scientific (Chicago, IL). All solutions were prepared with distilled deionized water. The channel flowrate, \dot{V} , was 0.5 mL/min and the cross flowrate, \dot{V}_c , was 3.2 mL/min.

The purified proteins BSA (98% monomer, MW = 67 kDa, pI 4.8) and γ -globulin (human, from Cohn Fraction II, III; 99% purity, MW = 156 kDa, pI 6.85–6.95) were obtained from Sigma Chemical Co (St. Louis, MO). Sample concentrations were 1.9 mg/mL for BSA and 2.7 mg/mL for γ -globulin. All protein solutions were prefiltered through $0.22 \text{ }\mu\text{m}$ membranes (Millipore, Billerica, MA). The injected sample volume was 10–20 μL . The eluted proteins were monitored using a UV detector set at a wavelength of 280 nm. The relative standard deviation of the retention time and peak area measurements did not exceed 3% and 10%, respectively.

Absolute sample recovery was calculated from the ratio of the protein amount eluted from the FIFFF channel to the protein amount injected [16, 17]. The latter

was determined from the peak area of a sample injected into the detector. A ~ 1 mL dilution tube was used in lieu of the FIFFF channel to maintain the same injected sample concentration as that used in a FIFFF analysis and obtain on-scale detector peaks. The resulting peak area represents the protein amount *injected* or 100% sample recovery. The protein amount *eluted* was calculated from the area of the sample peak that was retained and eluted from the FIFFF channel.

2.4 Results and Discussion

2.4.1 Asymmetric FIFFF (AsFIFFF) of Lactate Dehydrogenase

Flow FFF comes in different variants that include the original symmetrical channel, the most frequently used asymmetric channel, and the most recently introduced hollow fiber channel. Numerous papers have been published on the application of these different variants to proteins and complexes, polysaccharides, nanoparticles, cellular components, cells, and micron-sized particulates [1–14].

Lactate dehydrogenase (LDH) is a good sample for illustrating the use of AsFIFFF to monitor relative changes. LDH-5 is an isoenzyme derived from the rabbit skeletal muscle. It consists of four similar polypeptide chains (M_4) with a total molecular weight of 140,000 Da ($4 \times 35,000$ Da) and an isoelectric point of ~ 7.5 . Figure 2.2 shows the effect of pH on the dissociation of LDH-5. At pH 7.6, the

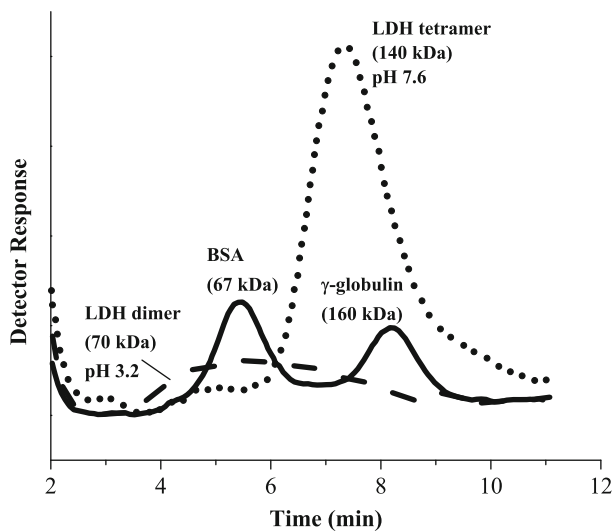


Fig. 2.2 AsFIFFF fractograms showing effect of pH on the formation of lactate dehydrogenase dimers and tetramers

tetramer form of LDH dominates and a large peak is observed at approximately 7.5 min. After suspending the LDH-5 in pH 3.2 buffer for 72 min, the enzyme has mostly dissociated into dimers and a broad fractogram with a peak maximum at ~5.5 min is obtained. The bovine serum albumin (BSA) and γ -globulin fractogram shown superimposed in Fig. 2.2 confirm the elution positions for the LDH-5 dimer (70 kDa) and tetramer (140 kDa).

The rate at which dissociation occurs was dependent on pH with faster dissociation under increasingly acidic conditions. At pH 5.0, the tetramer peak does not show any significant change at the 37 min mark. However, a significant shift in retention time is observed in pH 3.2 buffer after the same amount of time had elapsed. The LDH dissociation was also observed to be a reversible process with reformation of the tetramer when the pH was increased from 4.0 to 6.7. This example demonstrates the gentleness of FIFFF and its suitability for monitoring changes in protein complexes.

2.4.2 Evaluating Membrane Performance Using FIFFF

Controlling protein–membrane interaction is a critical component in the optimization of ultrafiltration (UF) processes [18] and flow FFF analyses. The strength (intensity) of the interaction is a complex function of many parameters such as membrane chemistry and morphology [19], protein structure [20], solution composition [21], and mechanism of protein transport to the membrane surface [22]. Due to this complexity, each protein–membrane pair would ideally be experimentally studied individually. In the case of ultrafiltration with fully retentive membranes, one has to also deal with several concurrent processes causing progressive reduction in system performance, e.g., concentration polarization, deposition of protein aggregates onto the membrane surface, and membrane pore constriction and blockage [23]. As a consequence, UF optimization experiments are very time and sample consuming, and data are difficult to correlate with original parameters affecting protein–membrane interaction.

A number of studies have evaluated other techniques, which are capable of providing more direct information about protein–membrane interaction, as tools for UF optimization. For instance, the study of protein adsorption on the membrane in static conditions [24] and direct measurements of intermolecular forces between a protein and a surface [25] have allowed the comparison of different UF membranes and showed good agreement with UF experiments. The limitation of these approaches as tools for UF optimization is the absence of UF hydrodynamic conditions. During UF, trans-membrane and tangential flow streams affect protein transport to a membrane surface, and hence, the strength of protein–membrane interactions [26]. This is analogous to the effect of cross and channel flowrates in FIFFF [16, 17].

One approach to the study of protein-membrane interactions is to examine the initial stage of protein adsorption onto a pristine membrane. It has previously been

observed that protein membrane interactions during the initial stage of UF have dramatic influence on long-term membrane performance [21]. At this initial stage, the main characteristic of protein–membrane interaction that should be measured is the amount of protein attached to the membrane surface or the initial protein surface coverage. On-line measurements have been made using a stirred cell UF module that was installed into a liquid chromatography system in place of a column [27]. A protein sample was injected and protein passing through a membrane was registered with an UV detector. Unfortunately, the enormous sample dilution experienced in the UF module resulted in very broad UV signals, making it difficult to determine the protein quantities.

This work describes an alternative approach to studying protein-membrane interactions, namely flow field-flow fractionation (FIFFF). During the FFF process, the protein sample moves along the membrane length and undergoes multiple interactions with the membrane surface. Repulsive interactions lead to shorter retention times t_r than theoretically predicted [16]. The opposite is true for attractive interactions, which in the extreme case results in irreversible sample adsorption. FIFFF can thus be used to study a range of weak to strong analyte-membrane interactions. The FIFFF channel hydrodynamics resembles that of a flat cross-flow UF module and the interactions that occur between a protein and a clean membrane can be associated with the very initial stage of UF. The advantage of this method compared to the method of [27] is that the sample dilution is sufficiently lower and protein signals are well-shaped peaks that can be easily characterized.

The application of FIFFF for studying analyte-membrane interactions is not yet widely recognized by FFF practitioners but has made inroads in the membrane filtration community. Published UF papers have demonstrated quantitative measurements of membrane fouling by organics, colloids, and microorganisms present in natural and waste waters and experimental verification of theoretical models [28–36]. To date, no UF publication has addressed quantitating protein fouling on membranes using FIFFF. Although a number of FIFFF papers have discussed approaches to reducing sample adsorption to the membrane as part of methods development [16, 17, 37–42], there has been no report of the purposeful use of FIFFF to quantitate protein recovery. The objectives of this study are to demonstrate the suitability of FIFFF as a tool to rapidly evaluate membrane performance. The results can then be applied to the optimization of FIFFF, UF, and other techniques where protein-membrane interactions must be controlled.

2.4.2.1 Effect of pH

FIFFF experiments were carried out for two globular proteins, six UF membranes, and six solution pHs in the range of 7.3–9.0. The same flowrates \dot{V} and \dot{V}_c were used for all experiments unless otherwise specified. The diluted 0.01 M Tham-boric acid buffer was chosen to reduce hydrophobic interactions between the membrane surface and protein molecules [21]. The pH of this buffer can be varied in the range of 7.3–9.0. Extension of pH range <7.3 would require the addition of

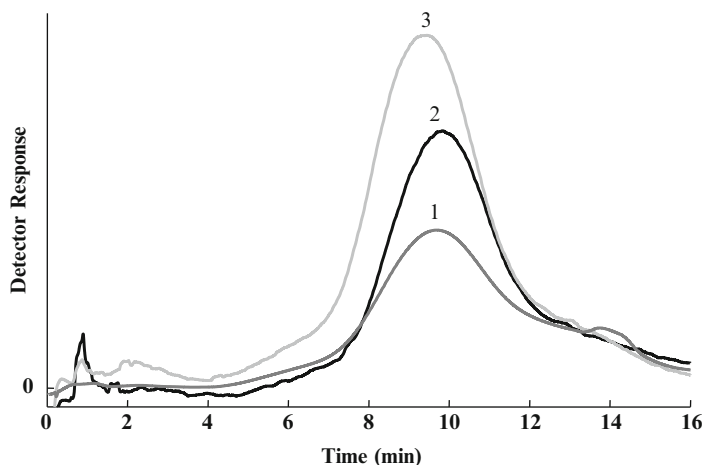


Fig. 2.3 FIFFF fractograms showing peak areas of γ -globulin obtained at different carrier liquid pH using the RC1 membrane

other chemicals, which would introduce new variables affecting the adsorption mechanism.

Typical FIFFF fractograms obtained for γ -globulin at different carrier liquid pHs are presented in Fig. 2.3. Each run was completed within 20 min.

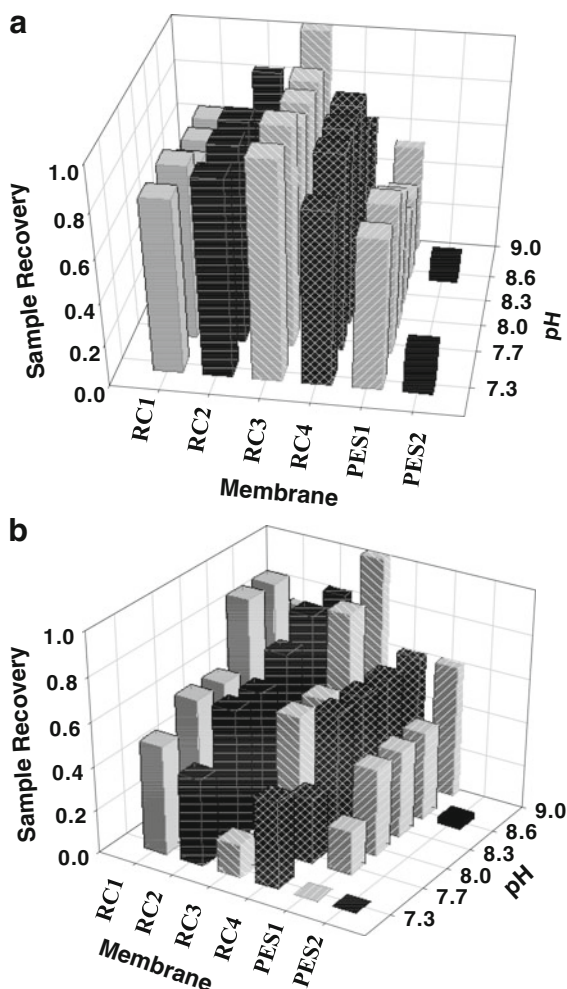
The peak areas are equated to sample recovery as described in the experimental section. Data obtained for the recovery of BSA and γ -globulin at different pH solutions (constant flowrates) are presented in Fig. 2.4. It is evident that sample loss occurred at most pHs studied.

The isoelectric points (pI) of the PES and RC UF membranes are about 3.1 and 3.4, respectively [43, 44]. The isoelectric point of BSA, (pI = 4.8), is sufficiently far from the studied pH range for one to expect strong electrostatic repulsion between protein molecules and both types of membrane. But even for these conditions, BSA recovery did not usually reach 100% (Fig. 2.4a). The isoelectric point of γ -globulin is in the range of 6.85–6.95. For all membranes, a decreasing γ -globulin recovery was observed as the pH approached the pI (Fig. 2.4b). This result is as expected. Structurally “soft” proteins, e.g., globular proteins BSA and γ -globulin, tend to have the highest adsorption onto various surfaces at a pH close to pI [20]. This phenomenon was also observed in UF experiments [21, 45].

2.4.2.2 Membrane Composition

In addition to the effect of solution pH, a significant influence of membrane chemistry on recovery was observed. The PES membranes tested in this study yielded substantially lower sample recoveries than the RC membranes for both BSA and γ -globulin. A similar result was also observed in UF studies [44]. This effect was likely caused by

Fig. 2.4 Recovery of (a) BSA and (b) γ -globulin from a FIFFF channel assembled with UF membranes of different chemistries and obtained from different sources. RC is regenerated cellulose and PES is polyethersulfone. $\dot{V} = 0.5$ mL/min, $\dot{V}_c = 3.2$ mL/min



the higher hydrophobicity of PES membranes. The PES repeat unit contains hydrophobic aromatic groups whereas the RC is more hydrophilic due to presence of hydroxyl groups. The increase in protein adsorption with increasing membrane hydrophobicity was also observed in a number of UF studies [26, 45].

Figure 2.4 also demonstrates that membranes with the same nominal surface chemistry from different suppliers can yield dramatically different protein recoveries. This is likely due to different membrane fabrication processes that result in different residual chemical functionalities at the surface, layered constructions, and surface roughness [16, 46]. These results emphasize the importance of performing preliminary experiments such as those described here to evaluate and establish a baseline for membrane performance and as part of methods development.

2.4.2.3 Proximity of Sample to Membrane Surface

Additional insights can be extracted from FIFFF fractograms. The measured retention time at peak maximum is related to the equilibrium mean layer thickness ℓ and flowrates as stated in Eq. 2.1. The higher the \dot{V}_c , the higher the t_r , the smaller the ℓ , the closer the analyte is to the membrane during the FIFFF separation. The opposite relationship holds for \dot{V} . Figure 2.5 is a plot of relative sample recovery versus ℓ . Here, the relative sample recovery is defined as the peak area relative to that measured for $\dot{V}_c = 2.75$ mL. $D_{BSA} = 6 \times 10^{-7}$ cm²/s [47] was used in calculating ℓ . Different t_r s and ℓ s were obtained when \dot{V}_c was varied (2.75, 3.21, 3.82, and 4.20 mL/min) while keeping \dot{V} constant at 0.5 mL/min. The data shows the highest sample recovery for $\ell > \sim 11$ μ m and complete sample loss for ℓ of 8 μ m. This set of experiments suggests that a threshold ℓ exists (for a specific analyte, solution, FIFFF channel dimensions, and membrane) and that ℓ can be used as a guide for selecting a \dot{V} and \dot{V}_c combination that is optimized for both resolution and sample recovery. Since ℓ is proportional to the ratio of the channel flowrate to cross flowrate, this ratio or the flow velocity equivalent $< v > / v_c$ can also be used to establish a threshold for optimized sample recovery as shown in Fig. 2.5b. Since sample recovery is dependent on both the channel and crossflows, a more complete picture can be obtained when their flowrate or flow velocity ratio is varied. The use of flow velocities removes the dependence on channel dimensions. Finally, since ℓ is proportional to D and D is temperature dependent, temperature may also play a role in controlling sample-membrane interactions.

2.4.2.4 Sample Deposition Along Channel length

The total amount of sample deposited per unit area on the membrane is readily calculated from the measured FIFFF sample recovery (amount of protein deposited = amount protein injected – amount protein eluted). However, this quantity does not give information about the rate of sample deposition or its distribution on the membrane. The deposition rate can be estimated using semi-empirical equations developed for UF [48, 49] and modifying the FIFFF mass flux equation. Experimentally, the deposition rate has been observed to decrease as the sample progresses along the membrane due to sample loss and the associated decrease in sample concentration. A fluorescence analysis of n-benzoyl-staurosporine, adsorbed on an UF membrane during FIFFF and then extracted from different pieces of the membrane, showed a gradual decrease in the adsorbed drug amount along the membrane length [37]. No drug adsorption was evident beyond the first half of the FIFFF channel.

The results of the previous study may partially explain the constant BSA recovery measured for five hollow fiber channels with lengths between 15 and 47 cm [40]. If BSA mainly adsorbs to the first part of the channel and saturates available sites, increasing the channel length (keeping all else constant) would not have a significant effect in the amount recovered. Pre-saturating the membrane with at least 2 μ g egg phosphatidylcholine or liposomes was reported to yield $\sim 100\%$ sample recovery and negligible carry-over [41].

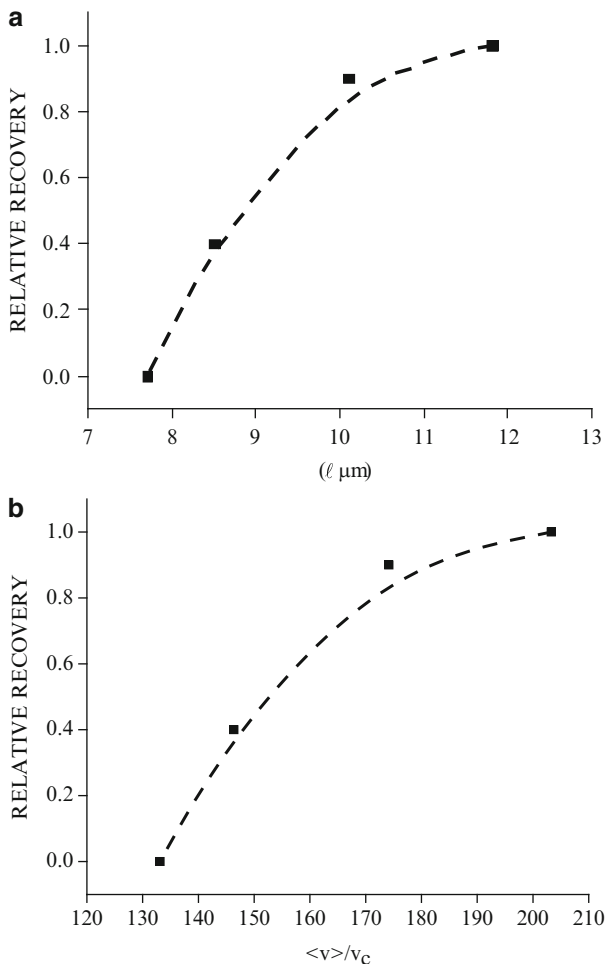


Fig. 2.5 Relative recovery of BSA as a function of (a) mean equilibrium distance ℓ from the regenerated cellulose wall and (b) the ratio of channel flow velocity $\langle v \rangle$ to crossflow velocity v_c . Channel dimensions are $28.4 \times 3.5 \times \sim 0.0254$ cm; carrier liquid is 0.01 M Tris-HCl, pH 7.2; $\dot{V} = 0.5$ mL/min. $\langle v \rangle = \dot{V}/bw$ and $v_c = \dot{V}_c/bL$ where b is channel breadth and L is length

2.5 Conclusion

Simple experiments have been described to study initial stage fouling on ultrafiltration membranes and to evaluate membrane performance for FIFFF. The pIs of the membrane and proteins and the pH of the solution should be taken in to consideration when selecting a carrier liquid. Other important factors such as membrane hydrophobicity, surface roughness, and batch-to-batch reproducibility are more difficult to control as these depend on the membrane manufacturers. However,

these parameters all culminate in the observed relationship between sample recovery and average distance of sample cloud to the membrane wall. The determination of a threshold ℓ can provide useful guidelines for selecting operating flowrates for both ultrafiltration and FIFFF analyses.

Acknowledgments The authors gratefully acknowledge support from the National Science Foundation CHE-1013029 and CBET-0968042.

References

1. Williams SKR, Runyon JR, Ashames AA (2011) Field-flow fractionation: addressing the nano challenge. *Anal Chem* 83:634–642
2. Yohannes G, Jussila M, Hartonen K, Riekkola ML (2011) Asymmetrical flow field-flow fractionation technique for separation and characterization of biopolymers and bioparticles. *J Chromatogr* 1218:4104–4116
3. Qureshi RN, Kok WT (2011) Application of flow field-flow fractionation for the characterization of macromolecules of biological interest: a review. *Anal Bioanal Chem* 399:1401–1411
4. Roda B, Zattoni A, Reschiglian P et al (2009) Field-flow fractionation in bioanalysis: a review of recent trends. *Anal Chim Acta* 635:132–143
5. Williams SKR, Lee D (2006) Field-flow fractionation of proteins, polysaccharides, synthetic polymers, and supramolecular assemblies. *J Sep Sci* 29:1720–1732
6. Andersson CI, Arfvidsson C, Kallio PT et al (2003) Enhanced ribosome and tRNA contents in *Escherichia coli* expressing a truncated *Vitreoscilla* hemoglobin mutant analyzed by flow field-flow fractionation. *Biotechnol Lett* 25:1499–1504
7. Lee H, Williams SKR, Allison SD et al (2001) Analysis of self-assembled cationic lipid-DNA gene carrier complexes using flow field-flow fractionation and light scattering. *Anal Chem* 73:837–843
8. Silveira JR, Raymond GJ, Hughson AG et al (2005) The most infectious prion protein particles. *Nature* 437:257–261
9. Yohannes G, Wiedmer SK, Hiidenhovi J et al (2007) Comprehensive two-dimensional field-flow fractionation-liquid chromatography in the analysis of large molecules. *Anal Chem* 79:3091–3098
10. Kim KH, Moon MH (2009) High speed two dimensional protein separation without gel by isoelectric focusing-asymmetrical flow field-flow fractionation: application to urinary proteome. *J Proteome Res* 8:4272–4278
11. McEvoy M, Razinkov V, Wei Z (2011) Improved particle counting and size distribution determination of aggregated virus populations by asymmetric flow field-flow fractionation and multiangle light scattering techniques. *Biotechnol Prog* 27:547–554
12. Arosio P, Barolo G, Muller-Spath T et al (2011) Aggregation stability of a monoclonal antibody during downstream processing. *Pharm Res* 28:1884–1894
13. Wahlund KG, Leeman M, Santacruz S (2011) Size separations of starch of different botanical origin studied by asymmetrical-flow field-flow fractionation and multiangle light scattering. *Anal Bioanal Chem* 399:1455–1465
14. Dubascoux S, Von Der Kammer F, Hecho L et al (2008) Optimisation of asymmetrical flow field-flow fractionation for environmental nanoparticles separation. *J Chromatogr* 1206: 160–165
15. Lundblad RL (2010) *Handbook of biochemistry and molecular biology*, 4th edn. CRC, Florida
16. Hartmann RL, Williams SKR (2002) Flow field-flow fractionation as an analytical technique to rapidly quantitate membrane fouling. *J Membr Sci* 209:93–106

17. Williams SKR, Giddings JC (2000) Sample recovery. In: Schimpf M, Caldwell K, Giddings JC (eds) FFF handbook. Wiley, New York
18. Zeman LJ, Zydney AL (1996) Microfiltration and ultrafiltration principles and applications. Marcel Dekker, Inc, New York
19. Matthiasson E (1983) The role of macromolecular adsorption in fouling of ultrafiltration membranes. *J Membr Sci* 16:23–36
20. Lyklema J, Norde W (1996) Interfacial behaviour of biomacromolecules. *Progr Colloid Polym Sci* 101:9–17
21. Fane AG, Fell CJD, Suki A (1983) The effect of pH and ionic environment on the ultrafiltration of protein solutions with retentive membranes. *J Membr Sci* 16:195–210
22. Cohen Stuart MA (1998) Chapter 1. In: Malmsten M (ed) Biopolymers at interfaces, vol 75, Surfactant science series. Marcel Dekker, New York, pp 1–25
23. Belfort G, Zydney AL (1998) Chapter 15. In: Malmsten M (ed) Biopolymers at interfaces, vol 75, Surfactant science series. Marcel Dekker, New York, pp 513–559
24. Amanda A, Mallapragada SK (2001) Comparison of protein fouling on heat-treated poly(vinyl alcohol), poly(ether sulfone) and regenerated cellulose membranes using diffuse reflectance infrared Fourier transform spectroscopy. *Biotechnol Prog* 17:917–923
25. Koehler JA, Ulbricht M, Belfort G (2000) Intermolecular forces between a protein and a hydrophilic modified polysulfone film with relevance to filtration. *Langmuir* 16:10419–10427
26. Marshall AD, Munro PA, Tragardh G (1993) The effect of protein fouling in microfiltration and ultrafiltration on permeate flux, protein retention and selectivity: A literature review. *Desalination* 91:65–108
27. Ghosh R, Cui Z (2000) Analysis of protein transport and polarization through membranes using pulsed sample injection technique. *J Membr Sci* 175:75–84
28. Kim S, Lee S, Kim CH, Cho J (2009) A new membrane performance index using flow-field-flow fractionation (fl-FFF). *Desalination* 247:169–179
29. Moon J, Lee S, Song J, Cho J (2010) Membrane fouling indicator of effluent organic matter with nanofiltration for wastewater reclamation, as obtained from flow field-flow fractionation. *Sep Purif Technol* 73:164–172
30. Pellegrino J, Wright S, Ranvill J, Amy G (2005) Predicting membrane flux decline from complex mixtures using flow-field-flow fractionation measurements and semi-empirical theory. *Water Sci Technol* 51:85–92
31. Moon J, Cho J (2005) Investigation of nano-colloid transport in UF membrane using flow field-flow fractionation (flow FFF) and an irreversible thermodynamic transport model. *Desalination* 179:151–159
32. Shon HK, Puntsho S, Chon K, Aryal R, Vigneswaran KIS, Cho J (2009) A study of the influence of ionic strength on the elution behaviour of membrane organic foulant using advanced separation tools. *Desalination Water Treat* 11:38–45
33. Kim DH, Moon J, Cho J (2005) Identification of natural organic matter (NOM) transport behavior near the membrane surface using flow field-flow-flow-fractionation (fl-FFF) micro channel. *J Water Supply Res T* 54:249–259
34. Lim SB, Lee SY, Choi S, Moon J, Hong SK (2010) Evaluation of biofouling potential of microorganism using flow field-flow fractionation (Fl-FFF). *Desalination* 264:236–242
35. Lee E, Shon HK, Cho J (2010) biofouling characteristics using flow field-flow fractionation: effect of bacteria and membrane properties. *Bioresource Technol* 101:1487–1493
36. Phuntsho S, Shon HK, Vigneswaran S et al (2011) Assessing membrane fouling potential of humic acid using flow field-flow fractionation. *J Membr Sci* 373:64–73
37. Madorin M, Van Hoogevest P, Hilfiker R et al (1997) Analysis of drug/plasma interactions by means of asymmetrical flow field-flow fractionation. *Pharm Res* 14:1706–1712
38. Li P, Hansen M, Giddings JC (1997) Separation of lipoproteins from human plasma by flow field-flow fractionation. *J Liq Chromatogr Relat Technol* 20:2777–2802
39. Lang R, Vogt L, Zurcher A et al (2009) Asymmetrical flow FFF as an analytical tool for the investigation of the physical stability of virus-like particles. *LC GC North Am* 27:844–852

40. Park I, Paeng KJ, Kang D et al (2005) Performance of hollow-fiber flow field-flow fractionation in protein separation. *J Sep Sci* 28:2043–2049
41. Hupfeld S, Ausbacher D, Brandl M (2009) Asymmetric flow field-flow fractionation of liposomes: 2. Concentration detection and adsorptive loss phenomena. *J Sep Sci* 32:3555–3561
42. Cao S, Pollastrini J, Jiang YJ (2009) Separation and characterization of protein aggregates and particles by field-flow fractionation. *Curr Pharm Biotechnol* 10:382–390
43. Pontie M, Chasseray X, Lemordant D, Laine MJ (1997) The streaming potential method for the characterization of ultrafiltration organic membranes and the control of cleaning treatments. *J Membr Sci* 129:125–134
44. Pontie M (1999) Effect of aging on UF membranes by a streaming potential (SP) method. *J Membr Sci* 154:213–220
45. Mockel D, Staude E, Guiver MD (1999) Static protein adsorption ultrafiltration behavior and cleanability of hydrophilized polysulfone membranes. *J Membr Sci* 158:63–75
46. Tsuyuhara T, Hanamoto Y, Miyoshi T et al (2010) Influence of membrane properties on physically reversible and irreversible fouling in membrane bioreactors. *Water Sci Technol* 61:2235–2240
47. Liu M-K, Li P, Giddings JC (1993) Rapid protein separation and diffusion coefficient measurement by frit inlet flow field-flow fractionation. *Protein Sci* 2:1520–1531
48. Ko MK, Pellegrino JJ, Nassimbene R, Marko P (1993) Characterization of the adsorption-fouling layer using globular proteins on ultrafiltration membranes. *J Membr Sci* 76:101–120
49. Ruiz-Bevia F, Gomis-Yagues V, Fernandez-Sempere J, Fernandez-Torres MJ (1997) An improved model with time-dependent adsorption for simulating protein ultrafiltration. *Chem Eng Sci* 52:2343–2352

Field-Flow Fractionation in Biopolymer Analysis

Williams, S.K.R.; Caldwell, K.D. (Eds.)

2012, X, 306 p., Hardcover

ISBN: 978-3-7091-0153-7